

# ***PTEN* losses exhibit heterogeneity in multifocal prostatic adenocarcinoma and are associated with higher Gleason grade**

Maisa Yoshimoto<sup>1</sup>, Keyue Ding<sup>2</sup>, Joan M Sweet<sup>3</sup>, Olga Ludkovski<sup>3</sup>, Greg Trottier<sup>4</sup>, Kyu S Song<sup>3</sup>, Anthony M Joshua<sup>5</sup>, Neil E Fleshner<sup>4</sup>, Jeremy A Squire<sup>1,2,6</sup> and Andrew J Evans<sup>3</sup>

<sup>1</sup>Department of Pathology and Molecular Medicine, Queen's University, Kingston, ON, Canada;

<sup>2</sup>NCIC Clinical Trials Group, Cancer Clinical Trials Division, Queen's University, Kingston, ON, Canada;

<sup>3</sup>Department of Pathology, Laboratory Medicine Program, University Health Network, Toronto General Hospital, Toronto, ON, Canada; <sup>4</sup>Division of Urology, Department of Surgical Oncology, Princess Margaret Hospital, Toronto, ON, Canada; <sup>5</sup>Department of Medical Oncology, Princess Margaret Hospital, Toronto, ON, Canada and <sup>6</sup>Barretos Cancer Hospital, Pio XII Foundation, Molecular Oncology Research Center, SP, Brazil

Prostatic adenocarcinoma is an epithelial malignancy characterized by marked histological heterogeneity. It most often has a multifocal distribution within the gland, and different Gleason grades may be present within different foci. Data from our group and others have shown that the genomic deletion of the phosphatase and tensin homolog deleted on chromosome 10 (*PTEN*) tumor suppressor gene and the disruption of the *ETS* gene family have a central role in prostate cancer and are likely to be associated with Gleason grade. In this study, prostate cancer samples were systematically analyzed to determine whether there was concordance between *PTEN* losses and *TMPRSS2-ERG* fusion rearrangements, within or between foci in multifocal disease, using well-annotated tissue microarrays (TMAs) consisting of 724 cores derived from 142 radical prostatectomy specimens. Three-color fluorescence *in situ* hybridization analysis of both the *PTEN* deletion and the *TMPRSS2-ERG* fusion was used to precisely map genetic heterogeneity, both within and between tumor foci represented on the TMA. *PTEN* deletion was observed in 56 of 134 (42%) patients (hemizygous = 42 and homozygous = 14). *TMPRSS2-ERG* fusion was observed in 63 of 139 (45%) patients. When analyzed by Gleason pattern for a given TMA core, *PTEN* deletions were significantly associated with Gleason grades 4 or 5 over grade 3 ( $P < 0.001$ ). Although *TMPRSS2-ERG* fusions showed a strong relationship with *PTEN* deletions ( $P = 0.007$ ), *TMPRSS2-ERG* fusions did not show correlation with Gleason grade. The pattern of genetic heterogeneity of *PTEN* deletion was more diverse than that observed for *TMPRSS2-ERG* fusions in multifocal disease. However, the marked interfocal discordance for both *TMPRSS2-ERG* fusions and *PTEN* deletions was consistent with the concept that multiple foci of prostate cancer arise independently within the same prostate, and that individual tumor foci can have distinct patterns of genetic rearrangements.

*Modern Pathology* (2013) 26, 435–447; doi:10.1038/modpathol.2012.162; published online 28 September 2012

**Keywords:** genomic biomarkers; histologic heterogeneity; index tumor; prognosis; *PTEN* gene; *TMPRSS2-ERG* fusion

Prostate cancer is widely recognized as being clinically and histologically heterogeneous,<sup>1–3</sup> with acinar type prostatic adenocarcinomas accounting for a vast majority of prostate cancers.<sup>4</sup> Prostate

cancer is also, most commonly, a multifocal disease at presentation,<sup>5</sup> and the morphologic appearance of these foci can be highly variable within a given prostate.<sup>3,6</sup>

The current approach to stratify risk for prostate cancer patients at the time of diagnosis relies heavily on the tumor grade in needle biopsies. The Gleason scoring system is the most widely used method for grading prostate cancer and is one of the most important predictors of tumor behavior.<sup>7,8</sup> Heterogeneity of prostate cancer within and between separate tumor foci with respect to the Gleason

Correspondence: Dr AJ Evans, MD, PhD, FRCPC, Department of Pathology, Laboratory Medicine Program, University Health Network, Toronto General Hospital, Eaton 11-444, 200 Elizabeth Street, Toronto, ON M5G 2C4, Canada.

E-mail: andrew.evans@uhn.ca

Received 19 December 2011; revised 30 July 2012; accepted 30 July 2012; published online 28 September 2012

pattern is well appreciated.<sup>9</sup> This heterogeneity along with sampling errors inherent in needle biopsies limits the accuracy of risk stratification, resulting in potential under- or overtreatment.<sup>10–12</sup> Increasing rates of prostate cancer detection, due to prostate-specific antigen screening,<sup>12</sup> underscore the need to improve our understanding of the molecular basis of the heterogeneity observed in this common cancer.

Genomic rearrangements leading to the formation of *TMPRSS2-ETS* gene fusions and deletion of the phosphatase and tensin homolog deleted on chromosome 10 (*PTEN*) tumor suppressor gene are the two most frequent alterations observed in prostate cancer.<sup>13–15</sup> The *TMPRSS2-ERG* gene fusion is the principle genomic alteration and a characteristic signature in approximately half of all prostate cancers.<sup>14,16–23</sup> *ERG* regulates matrix metalloproteinases, thus influencing extracellular matrix remodeling and the invasive potential of malignant cells.<sup>24–27</sup> *PTEN* is among the most commonly mutated tumor suppressor genes in human cancer.<sup>28</sup> *PTEN* targets proteins in signaling pathways that regulate cell growth, survival and genome stability. Inactivation of *PTEN* and its role in oncogenesis in human prostate cancer is well documented.

Early studies using loss of heterozygosity analyses of deletions of 10q showed that *PTEN* loss is present in 35–58% cases of advanced prostate cancers.<sup>29–31</sup> *PTEN* deletions are found in approximately 40% of localized prostate cancers.<sup>8,14,31–44</sup> In advanced disease, fluorescence *in situ* hybridization (FISH) has identified hemizygous (loss of one copy) and homozygous (loss of both copies) *PTEN* deletions,<sup>31,39,43,45,46</sup> with the incidence of *PTEN* deletion approaching 70–80% of castrate-resistant tumors.<sup>33,40,42,43</sup> It has been shown that hemizygous *PTEN* deletions are associated with earlier biochemical relapse. Homozygous *PTEN* deletions are strongly linked to metastasis and androgen-independent progression.<sup>20,33,39,40,47,48</sup> Genomic loss and inactivation of the *PTEN* gene most likely lead to an adverse clinical course through haploinsufficiency and reduced levels of the *PTEN* protein.<sup>49</sup> Loss of *PTEN* leads to upregulation of PI3K/AKT, a pathway strongly associated with disease progression in prostate cancer.<sup>40,48,50–52</sup> The *TMPRSS2-ERG* fusion gene, constituting the majority of *ETS* rearrangements in prostate cancer, likely has an important role in prostate cancer progression, as its promoter region drives the expression of the fused *ETS* gene.

Although there is an abundance of information on association of these genomic changes and clinical outcomes in prostate cancer, data on their distribution in multifocal disease and their relationships to individual Gleason grades are limited. Barry *et al*<sup>53</sup> demonstrated intrafocal homogeneity and interfocal heterogeneity for *TMPRSS2-ERG* rearrangements in radical prostatectomy specimens, but found no association between the Gleason score of a particular focus and the presence or absence of *TMPRSS2-ERG* rearrangements. Similar studies have not been

performed for *PTEN*. It is important to note that no study to date has specifically studied the relationship between *PTEN* and *TMPRSS2-ERG* status and individual Gleason patterns that are combined to give a Gleason score. To this end, we constructed a tissue microarray (TMA) from 142 radical prostatectomy specimens by obtaining cores of tumor from separate foci, with an emphasis on sampling specific Gleason patterns.

## Materials and methods

### Patient Cohort and Tumor Samples

A cohort of prostate cancer patients comprising 614 men who underwent both needle biopsy and radical prostatectomy at the University Health Network between 2000 and 2006 was used to select the cases for this study. Radical prostatectomy specimens at our institution are processed according to a standard protocol. The specimen is completely fixed in 10% formalin and serially sectioned at 3–4 mm intervals in a plane perpendicular to the urethra. The serial slices are divided into quadrants and submitted for histologic assessment. The blocking legend in the pathology report indicated the location from which specific sections were taken. All specimens were staged using the TNM classification. For this study, the radical prostatectomy specimens were reviewed and graded according to the 2005 modified International Society of Urological Pathology Gleason scoring system,<sup>8</sup> hereafter referred to as modified Gleason score, grade or pattern (Table 1).

### TMA Construction

All original H&E slides from 168 radical prostatectomy specimens obtained between 2000 and 2001 were reviewed to select samples for inclusion in the TMA. A final cohort of 142 cases was chosen based on availability of the appropriate paraffin blocks. Within each prostatectomy specimen, individual foci in specimens with multifocal prostate cancer were defined by the criteria of Mehra *et al*.<sup>54</sup> Cancer foci that were separated by  $\geq 3$  mm in a single section or separated by  $\geq 4$  mm in adjacent blocks (above or below) were considered as separate foci. Each focus of prostate cancer was measured on the slides to obtain the largest dimension. For foci that overlapped in two or more serial blocks, the block with the largest dimension for that focus was selected for analysis. The modified Gleason score for each focus was annotated on the glass slides, as were areas showing different Gleason patterns. In cases of multifocal disease, we limited our analyses to the largest focus and up to two of the next largest foci. Separate foci on opposite sides of the prostate were specifically chosen whenever possible. When there were  $\geq 3$  foci, those containing tumor with the highest modified Gleason patterns were targeted

**Table 1** Patient/pathology/outcome characteristics from a typical North American prostatectomy cohort (2000–2002)

|                                   |                |
|-----------------------------------|----------------|
| Age, years (range)                | 61.9 (44–77)   |
| Initial PSA, ng/ml (range)        | 7.0 (3.0–45.4) |
| <i>Radical prostatectomy data</i> |                |
| Gleason score                     |                |
| 6/10 (3 + 3)                      | 33 (23%)       |
| 7/10 (3 + 4)                      | 76 (54%)       |
| 7/10 (4 + 3)                      | 26 (18%)       |
| 8/10 (4 + 4)                      | 2 (1%)         |
| 9/10 (4 + 5)                      | 1 (<1%)        |
| 9/10 (5 + 4)                      | 4 (3%)         |
| Pathologic stage <sup>a</sup>     |                |
| pT2a                              | 6 (4%)         |
| pT2b                              | 7 (5%)         |
| pT2c                              | 96 (68%)       |
| pT3a                              | 23 (16%)       |
| pT3b                              | 10 (7%)        |
| Distribution of prostate cancer   |                |
| Multifocal                        | 112 (79%)      |
| Unifocal                          | 30 (21%)       |
| Surgical margins                  |                |
| Positive                          | 42 (30%)       |
| Negative                          | 100 (70%)      |

Abbreviation: PSA, prostate-specific antigen.

<sup>a</sup>Total number in cohort = 142. Regional lymph node dissections were performed in 13/109 (12%) pT2 cases, none of which showed lymph node involvement, and in 7/33 (21%) pT3 cases, 2 of which were positive for metastatic prostatic adenocarcinoma.

irrespective of their size. It was felt that this approach would optimize our ability to detect heterogeneity within and between separate foci.

To construct the TMA, up to three 0.6 mm cores were obtained from a given tumor focus and transferred to the recipient blocks. TMA cores were taken from different areas within each focus, separated by 5 mm where possible, to allow us to assess genomic heterogeneity within and between foci. Only one core was typically obtained from foci  $\geq 5$  mm. Within a given cancer focus, areas showing different modified Gleason patterns were specifically sampled. Using the above strategy, we attempted to include up to six cores from each prostatectomy specimen. Representative cores of non-tumor prostate tissue were included for control purposes. A summary of the sampling procedure used to construct the TMA is shown in Figure 1. The completed TMA included a total of 724 cores distributed over three separate recipient blocks. Five-micron H&E sections from each recipient block were reviewed before the FISH studies. Specifically, each TMA core was reviewed to verify the presence of adenocarcinoma and to annotate the modified Gleason grade of the tumor.

### ***TMPRSS2-ERG* Probe Design, Classification and FISH Analysis**

Sequential break-apart three-color FISH was used for studying the *TMPRSS2-ERG* gene rearrangement as previously described.<sup>14,15</sup> As the extension of the

gap between 3'-*ERG* and 5'-*ERG* signals depends on the spreading of the breakpoints, chromatin architecture and compaction, as well as the probe design, a reproducible scoring system was established for our break-apart FISH strategy. We have estimated the relative distance between the differentially colored probes of a signal pair within the nucleus as follows: (1) co-localized signals: distance between the 3'-*ERG* and 5'-*ERG* signals less than one signal diameter; (2) non-overlapping signals: distance between the 3'-*ERG* and 5'-*ERG* signals more than two times the estimated signal diameter.<sup>55</sup> Subsequently, the *TMPRSS2-ERG* rearrangement mechanisms were classified according to the pattern of interphase FISH signals.<sup>56</sup> Class N described the normal *ERG* locus; therefore, co-localization of the two *ERG* probe signals in close proximity to the *TMPRSS2* signal. Class Edel (fusion gene via interstitial deletion) described an interstitial deletion at cytoband 21q22.2-3 and was characterized by co-localization of the 3'-*ERG* and *TMPRSS2* signals and absence of the 5'-*ERG* signal. Class Esplit (fusion gene via structural rearrangement, eg, translocation) described a genomic rearrangement, leading to insertion of those sequences elsewhere in the genome to an unknown chromosome location, resulting in the separation of the 5'-*ERG* signals from the co-localized 3'-*ERG* and *TMPRSS2* signals. In both types of *TMPRSS2-ERG* rearrangements (Edel and Esplit), the unaffected chromosome 21 generally displayed a Class N signal configuration. Finally, Class 2 + Edel described additional copies of the *TMPRSS2-ERG* gene fusions.

In each TMA core, 50–100 non-overlapped, intact interphase tumor nuclei were scored for the presence/absence of the *TMPRSS2-ERG* gene fusion. A core was deemed technically inadequate for scoring if it lacked a diagnostic target tissue or was of weak non-interpretible probe signal. Digitally scanned adjacent H&E TMA sections were available for side-by-side comparison with the FISH image to confirm the location of tumor cells. Areas of modified Gleason grade 3, 4 or 5 tumor were analyzed using the break-apart three-color strategy, and were classified according to the aforementioned FISH signal patterns. On the basis of hybridization in control cores (benign prostatic epithelium, data not shown) and the tumor cohort, detection of the *TMPRSS2-ERG* rearrangement was considered to be present when a minimum of 10% of the counted cells contained an Esplit or a minimum of 20% of the cells contained an Edel in a given core.<sup>55</sup> A core was considered fusion-positive if any of its representative spots met the above cutoff values. The 10 (Esplit) and 20% (Edel) cutoff values were also reassessed by analyzing the percentage of fusion-positive nuclei in a given core, alongside the percentage of nuclei with normal signal for each core from the TMA. This reassessment of the cutoff values was particularly useful for cores exhibiting more cellular heterogeneity where cells differed in

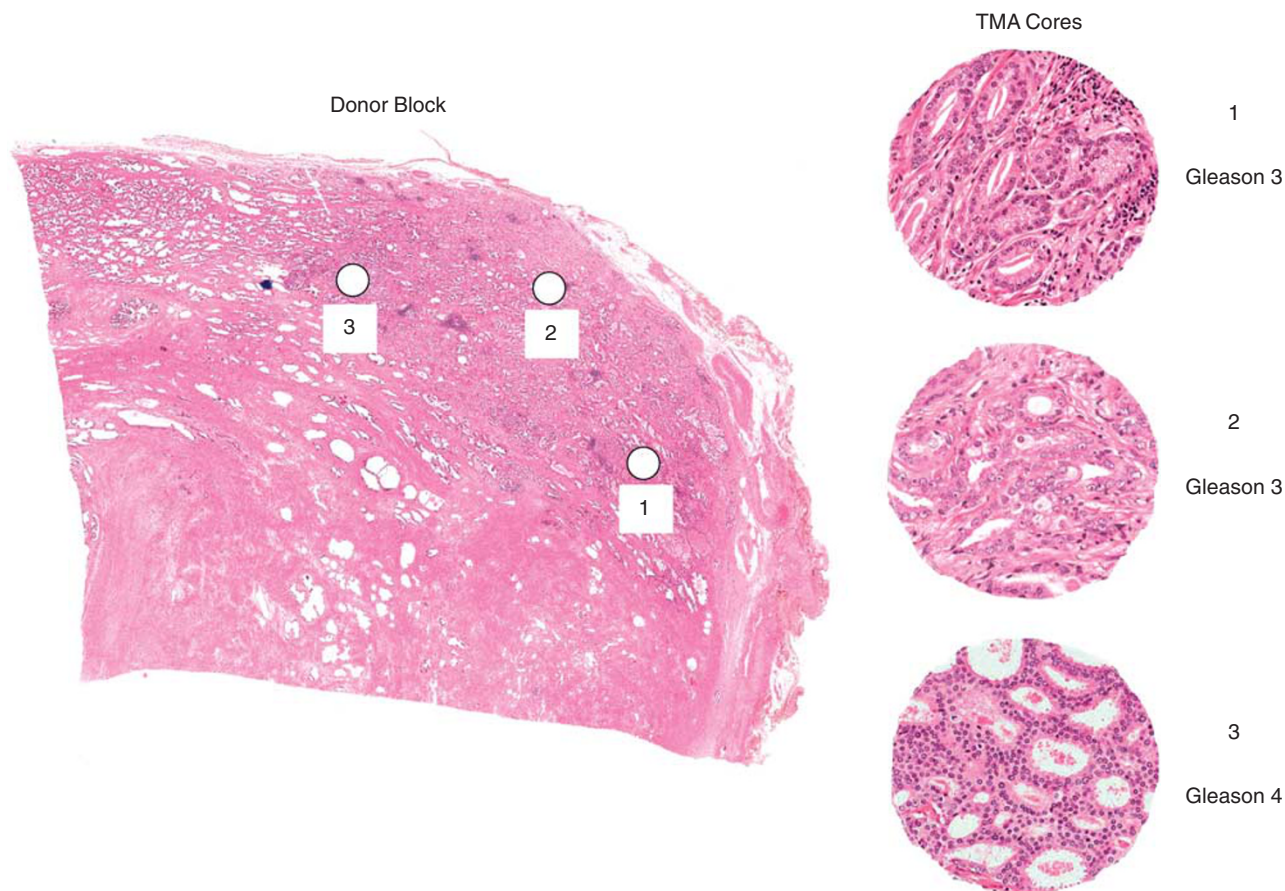


**Figure 1** Schematic showing sampling for tissue microarray (TMA) construction. Photomicrographs illustrating the protocol used to construct the TMA. The left side of the figure shows a low power overview of a typical donor block containing an index focus of adenocarcinoma. The locations of three representative 0.6 mm cores (1, 2 and 3) were annotated on the donor slide as shown. The resulting TMA cores are shown on the right, along with the Gleason patterns for the adenocarcinoma in each core. Wherever possible, cores showing different Gleason patterns were specifically sampled within a given focus.

shape, size or density. In majority of the cores, the relative percentage of fusion-negative *versus* fusion-positive cells was less extreme. In general, any inconsistent results were characterized by either poor nuclear morphology or truncation artifacts associated with histological sectioning. In addition, the presence of a copy-number gain of a non-rearranged *ERG* and/or *TMPRSS2* gene was simultaneously assessed in all evaluated nuclei in a given TMA core (data not shown).

#### ***PTEN* Probe Design and FISH Analysis**

A three-color FISH method was designed based on methods used previously by our group.<sup>44</sup> As described above, FISH analysis was performed using adjacent sections stained with DAPI (4',6-diamidino-2-phenylindole, dihydrochloride) in selected areas of adenocarcinoma. *PTEN* copy number was evaluated by counting spots for each probe in 50–100 non-overlapping, intact, interphase nuclei per tumor TMA core. Variation of nuclear size present in the three TMA blocks required that we use non-*PTEN*-

deleted prostate cancer cores as controls to define the threshold for classifying the *PTEN* copy number.<sup>44</sup> Background information on the assay and on determining cut-off thresholds is also available on our web site ([www.ptendeletion.net](http://www.ptendeletion.net)). Overall, the mean + 3 s.d. was used as the cutoff value for assigning hemizygous deletion status (>45%) in each array. As with the *TMPRSS2-ERG* FISH described above, this approach was particularly useful for cores exhibiting more cellular heterogeneity where cells differed in shape, size or density. Homozygous deletion status for *PTEN* was defined by more conservative criteria, a simultaneous lack of both *PTEN* locus signals<sup>55,57–59</sup> in >30% of scored nuclei.<sup>58</sup> In addition, TMA cores with inconclusive results or high degree of heterogeneity were reevaluated/rescored using a whole formalin-fixed paraffin-embedded section from the original donor block.

#### **Heterogeneity Index**

To explore the pattern of genomic change within and between tumor foci in each prostatectomy

specimen, a heterogeneity index<sup>60</sup> was used to determine whether high or low rates of *PTEN* loss and/or *TMPRSS2-ERG* fusion were associated with modified Gleason pattern. For each sample, the heterogeneity index for *PTEN* and *TMPRSS2-ERG* fusion was calculated as a ratio of the number of different patterns of *PTEN* (no *PTEN* deletion, hemizygous and homozygous *PTEN* deletion) and *TMPRSS2-ERG* fusion signals (Class N, Class Edel, Class Esplit) divided by the total number of analyzed foci from each prostatectomy specimen. Thus, *PTEN* and *TMPRSS2-ERG* FISH patterns presented different heterogeneity levels. For example, the *PTEN* heterogeneity index ranged from 0.2 to 2.0, and the *TMPRSS2-ERG* heterogeneity index ranged from 0.1 to 2.0. The visualization of heterogeneity index data set was performed using the Multi Experiment Viewer software.<sup>61</sup>

### Statistical Analyses

On the basis of a pre-specified statistical analysis plan, exploratory analyses were performed to characterize relationships between the incidences of *PTEN* deletion (homozygous or hemizygous losses) and *TMPRSS2-ERG* fusion (Esplit or Edel) as determined by FISH and modified Gleason pattern in adjacent prostatectomy sections. The  $\chi^2$ -test was used to test for association between FISH biomarkers and modified Gleason pattern, based on an expected frequency assuming random distribution of each class. All reported *P*-values are two-sided, and a level of 5% (*P*=0.05) was considered to be statistically significant.

## Results

### Patient Characteristics

The characteristics of the patients included in this study are shown in Table 1. The study set represents a typical North American radical prostatectomy cohort in terms of age, serum prostate specific antigen at time of diagnosis, distribution of modified Gleason scores, distribution of disease within the prostate (multifocal vs unifocal), pathologic stage and margin positivity. As would be expected in a cohort treated by radical prostatectomy with curative intent where most prostate cancers were found through prostate-specific antigen testing, the proportion of cases having Gleason scores of 8–10/10 was low (<5%). Pelvic lymph node dissections were performed in 20/142 patients (14%) with 2/20 (10%) being positive for metastatic prostatic adenocarcinoma.

### Multifocality of Modified Gleason Grade in Study Group

Although the TMA comprised 742 cores, review of H&E sections of the TMA revealed that only 692 cores (93%) contained adequate tumor for analysis,

517 (70%) of which contained modified Gleason pattern 3 tumor, 169 (23%) contained modified Gleason pattern 4 tumor, and 6 (1%) contained modified Gleason pattern 5 tumor. These cores represented 510 separate tumor foci from 139 of 142 prostatectomy specimens (98%). The mean number of foci per specimen was 3.6 (range 1–6). Of these 139 cases, 5 additional cases could not be evaluated by *PTEN* FISH because of loss of TMA cores, an insufficient number of tumor nuclei in the TMA cores and/or technical failure of the FISH. This left a total of 567 cores from 134 radical prostatectomy specimens. All 139 cases could be evaluated by *TMPRSS2-ERG* FISH.

### Overall Frequencies of *PTEN* Deletion and *TMPRSS2-ERG* Fusion Gene

Overall, *PTEN* deletion was observed in 56 of 134 (42%) of the evaluable prostatectomy cases (hemizygous = 42 and homozygous = 14) and *TMPRSS2-ERG* fusion was observed in 63 of 139 evaluable cases (45%; Table 2). Considering the total number of 134 cases assessed for *PTEN*, 19 cases (14%), from the previously described 56 cases with *PTEN* deletion, showed *PTEN* deletion within at least one tumor focus, whereas 76 of 134 (57%) prostatectomies appeared to have the normal two copies of *PTEN* in all tumor foci (Supplementary Table 1).

In total, 10 of 139 (7%) prostatectomy cases showed *TMPRSS2-ERG* fusion gene within at least one tumor focus, whereas 76 of 139 (55%) cases

**Table 2** Summary of the *PTEN* deletion and *TMPRSS2-ERG* fusion in prostatic adenocarcinomas RP samples by FISH

| <i>FISH</i> results  | No. of samples/total radical prostatectomies <sup>a</sup> |
|--|---|
| <i>PTEN</i> not deleted (%)                                | 78/134 (58)   |
| Hemizygous <i>PTEN</i> deletion (%)                        | 42/134 (31)   |
| Homozygous <i>PTEN</i> deletion (%) <sup>b</sup>           | 8/134 (6)   |
| Hemi- and homozygous <i>PTEN</i> deletion (%) <sup>b</sup> | 6/134 (4)   |
| <i>TMPRSS2-ERG</i> Class N (%) <sup>c</sup>                | 77/139 (55)   |
| <i>TMPRSS2-ERG</i> Class Edel (%) <sup>d</sup>             | 40/139 (29)   |
| <i>TMPRSS2-ERG</i> Class Esplit (%)                        | 21/139 (15)   |
| <i>TMPRSS2-ERG</i> Class Edel and Esplit (%)               | 1/139 (<1)  |

Abbreviation: FISH, fluorescence *in situ* hybridization; *PTEN*, phosphatase and tensin homolog deleted on chromosome 10. Class Esplit is characterized by the co-localization of the 3'-*ERG* and *TMPRSS2* signals, with the retention of the 5'-*ERG* signal elsewhere in the nucleus.

<sup>a</sup>*PTEN* FISH analysis were not suitable for all 139 radical prostatectomies specimens.

<sup>b</sup>These two classes of *PTEN* deletion were combined as homozygous deletion.

<sup>c</sup>Class N, where no *ERG* rearrangement has occurred.

<sup>d</sup>Class Edel is characterized by the co-localization of 3'-*ERG* probe to the *TMPRSS2* probe signals, and the absence of the 5'-*ERG* signal. This represents rearrangement with the loss of the intervening sequence.

appeared to have no *TMPRSS2* fusion gene in any of the tumor foci examined. We observed class Edel *TMPRSS2* fusion gene in 40 of 139 (29%) of the cases examined. Esplit class *TMPRSS2-ERG* fusion genes were present in 21 of 139 (15%) cases (Table 2 and Figure 2).

After acquisition of FISH data, the cases were reviewed to search for potential associations between *PTEN* deletion and *TMPRSS2-ERG* rearrangements. We, therefore, examined the differential status of *PTEN* (deleted or not deleted) and the presence of *TMPRSS2-ERG* fusion in 132 cases where a complete evaluation was possible. In 32 of 132 prostatectomies (24%), concurrent *PTEN* loss and *TMPRSS2-ERG* fusion gene was observed (Table 3).

### *PTEN* Deletions and *TMPRSS2-ERG* in Different Gleason Patterns

The occurrence of genomic heterogeneity within individual cancer foci in this cohort allowed us to carefully document core-by-core variation using FISH and examine any associations between *PTEN* loss or *TMPRSS2-ERG* fusion gene rearrangement and modified Gleason pattern. In addition, we performed an analysis of the relative levels of genetic heterogeneity of both classes of genomic alteration. An example of this genomic heterogeneity is shown in Figure 3. The foci on the right side of the gland showed two deletion patterns for *PTEN*—hemizygous deletion in core 2 and homozygous

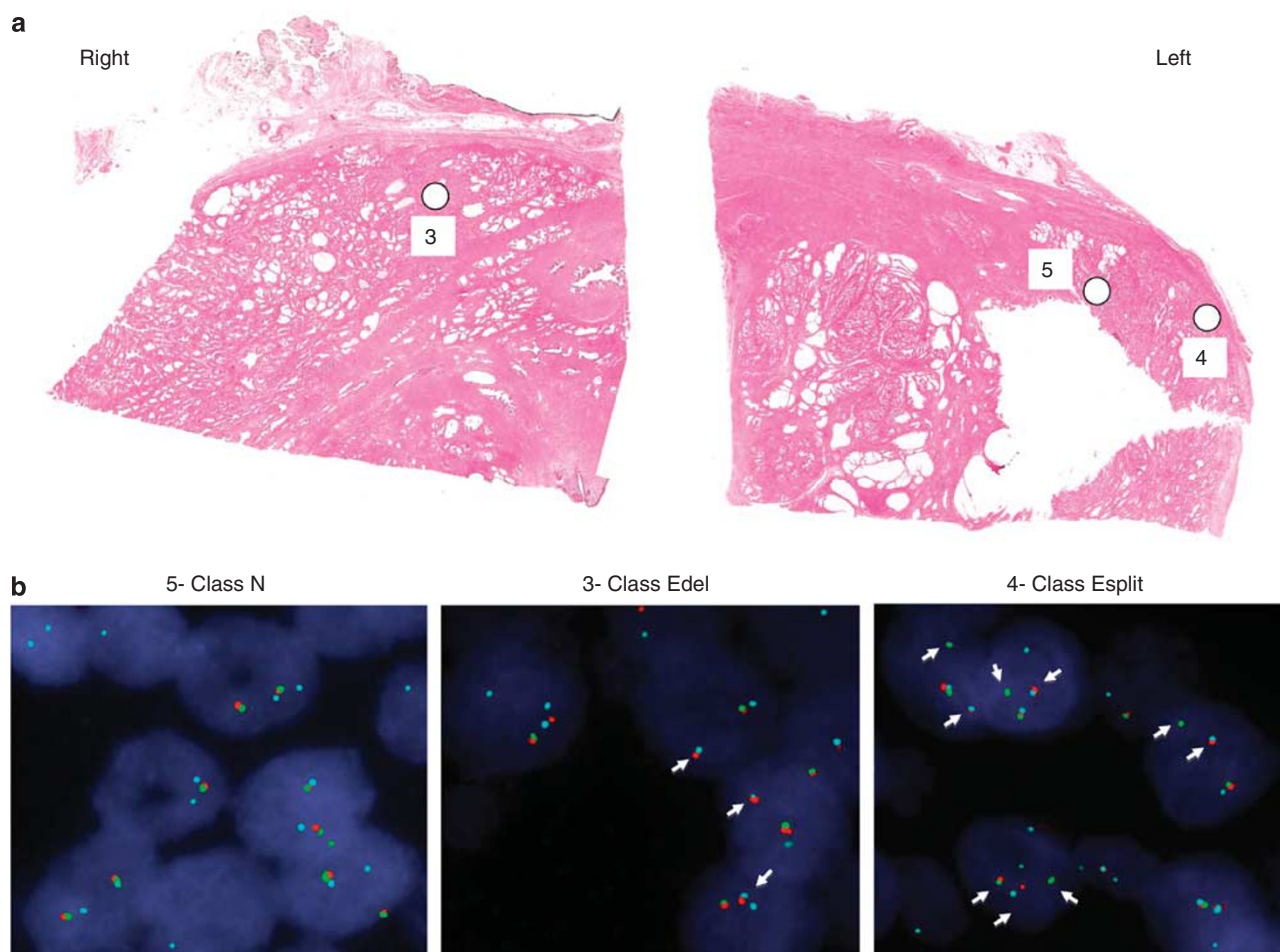


**Figure 2** Representative example of *TMPRSS2-ERG* heterogeneity in multifocal prostate cancer. (a) Hematoxylin and eosin sections from the right posterior and left anterior quadrants of a radical prostatectomy specimen with separate foci of adenocarcinoma showing the locations from which tissue microarray (TMA) cores were obtained. (b) Representative pseudo-colored three-color FISH images of prostate cancer formalin-fixed paraffin-embedded TMA cores. Color key: red, 3'-*ERG*; green, 5'-*ERG*; pale blue, *TMPRSS2*. Nuclei are counterstained with DAPI (4',6-diamidino-2-phenylindole, dihydrochloride). The original magnification is  $\times 63$ . The image on the left displays a Class N tumor core derived from the focus 5 (Gleason 3). No *ERG* rearrangement has occurred, where co-localization of 3'- and 5'-*ERG* probes with the 5'-*TMPRSS2* bacterial artificial chromosome probe signals (red) indicate a normal Chr21q22.2-3 locus. The following image displays a Class Edel tumor core derived from the focus 3 (Gleason 3), which is characterized by the co-localization of 3'-*ERG* probe to the *TMPRSS2* probe signals, and the absence of the 5'-*ERG* signal. This represents rearrangement with the loss of the intervening sequence. The unaffected Chr21 displays Class N configuration. The image on the right displays a Class Esplit, which is a tumor core derived from the focus 4 (Gleason 3) characterized by the co-localization of the 3'-*ERG* and *TMPRSS2* signals, with the translocation of the 5'-*ERG* signal. The unaffected Chr21 displays Class N configuration.

**Table 3** Distribution of RP tumors showing *PTEN* deletion and *TMPRSS2-ERG* fusion in prostatic adenocarcinomas

| <i>TMPRSS2-ERG</i> fusion | <i>PTEN</i> |          |
|---------------------------|-------------|----------|
|                           | No deletion | Deletion |
| Absence (%)               | 48 (37)     | 24 (18)  |
| Presence (%)              | 28 (21)     | 32 (24)  |

Abbreviation: *PTEN*, phosphatase and tensin homolog deleted on chromosome 10.

deletion in core 3. In contrast, neither of the cores taken from the separate cancer focus on the left side of the gland showed *PTEN* deletion. With respect to *TMPRSS2-ERG*, the normal configuration was the predominant pattern in this case, with only core 2 on the right side having tumor cells with a Class Edel configuration.

Six of 134 (5%) cases showed genomic heterogeneity with respect to the extent of *PTEN* deletion, with both hemizygous and homozygous loss being observed in separate tumor foci from the same prostate (Table 2). In the 56 *PTEN*-deleted cases, uniform mechanisms of deletion were seen in all cancer foci examined in only 5 of the 56 (9%) cases. In four (3%) of these cases, hemizygous *PTEN* losses were present in all tumor foci examined.

In one case (1%) genomic heterogeneity was evident, with both mechanisms of the *TMPRSS2-ERG* fusion gene rearrangement being observed in separate tumor foci within the same prostate gland. In 62 *TMPRSS2-ERG* fusion-positive cases, the same mechanism of fusion gene formation was seen in 9 of the 62 cases (15%) in all cancer foci. The relative levels of genomic heterogeneity in the cohort is presented in Figure 4 (derived from Supplementary Table 1), which allows for a direct comparison of the pattern genomic diversity for *PTEN* deletion with that observed for the *TMPRSS2-ERG* fusion. The observed interfocal discordance for both *TMPRSS2-ERG* fusions and *PTEN* deletions demonstrated that individual tumor foci can have distinct patterns of both genetic rearrangements. Moreover, despite the differing sensitivities and specificities of both FISH assays in relation to truncation losses, it can be seen that both inter- and intrafocal diversity for *PTEN* genomic change (hemizygous loss or homozygous loss) is much greater than that observed for *TMPRSS2-ERG* fusions (Esplit or Edel).

Figure 5 compares the diversity of genomic change within individual foci for *PTEN* and *TMPRSS2-ERG* fusion using a heterogeneity index. For each sample, the heterogeneity for *PTEN* and *TMPRSS2-ERG* fusion was calculated as a ratio of the number of different patterns of *PTEN* (no *PTEN* deletion, hemizygous and homozygous *PTEN* deletion) and *TMPRSS2-ERG* fusion signals (Class N, Class Edel, Class Esplit) divided by the total number of foci analyzed for each prostatectomy specimen. The

metric was then used to determine whether high or low rates of *PTEN* deletion or *TMPRSS2-ERG* fusion were associated with the specific modified Gleason pattern present in a given TMA core. It can be seen that greater indices of heterogeneity for *PTEN* are associated with higher modified Gleason patterns, with that for pattern 4 or 5 (higher) being greater than that for pattern 3 (lower). Conversely, we found no relationship between the *TMPRSS2-ERG* fusion and modified Gleason pattern.

Our TMA design allowed us to statistically evaluate associations between *PTEN* deletion and *TMPRSS2-ERG* and cancer foci bearing different modified Gleason patterns. In Table 4, a  $\chi^2$ -analysis of 692 individual TMA cores showed greater-than-expected association between *PTEN* loss and modified Gleason pattern 4 ( $P < 0.001$ ). In contrast, there was no association between the presence or absence of *TMPRSS2-ERG* fusions and modified Gleason pattern. However, when individual cores were compared (Table 5) by  $\chi^2$ -analysis, there was a greater-than-expected association between *PTEN* loss and the presence of the *TMPRSS2-ERG* fusion gene ( $P = 0.007$ ).

## Discussion

The relationship between genomics and morphology in multifocal prostate cancer is not well understood. Multifocal prostate cancer generally consists of a predominant focus and one or more separate smaller foci.<sup>5,9,62,63</sup> It has been estimated that between 50–80% of prostates have more than one tumor focus at the time of diagnosis.<sup>3,64,65</sup> Moreover, multifocal prostate cancer frequently shows histologic heterogeneity, with separate tumor foci exhibiting different Gleason scores (reviewed in Andreoiu and Cheng<sup>3</sup>, Arora *et al*,<sup>9</sup> Mehra *et al*,<sup>9</sup> and Ruijter *et al*<sup>63</sup>). Identifying the cancer focus in multifocal disease that determines clinical behavior for an individual patient is an important but problematic issue. The largest focus has historically been defined as the ‘index tumor,’ which has also been assumed to be the one that determines clinical behavior.<sup>66,67</sup> More recent evidence has challenged this definition in that the largest tumor focus does not always contain the highest Gleason score or pathologic stage, and several studies have failed to show independent prognostic significance for the largest tumor focus (reviewed in Andreoiu and Cheng<sup>3</sup>). Participants in the 2009 International Society of Urological Pathologists Consensus Conference on the Handling and Staging of Radical Prostatectomy Specimens were unable to reach a consensus definition for the term ‘index tumor’ based on histopathology alone. It was felt that the definition should be context-dependent, taking differences in Gleason score and pathologic stage of individual foci into account to identify the index tumor.<sup>68</sup> Genomic and/or cytogenetic characterization of different foci in

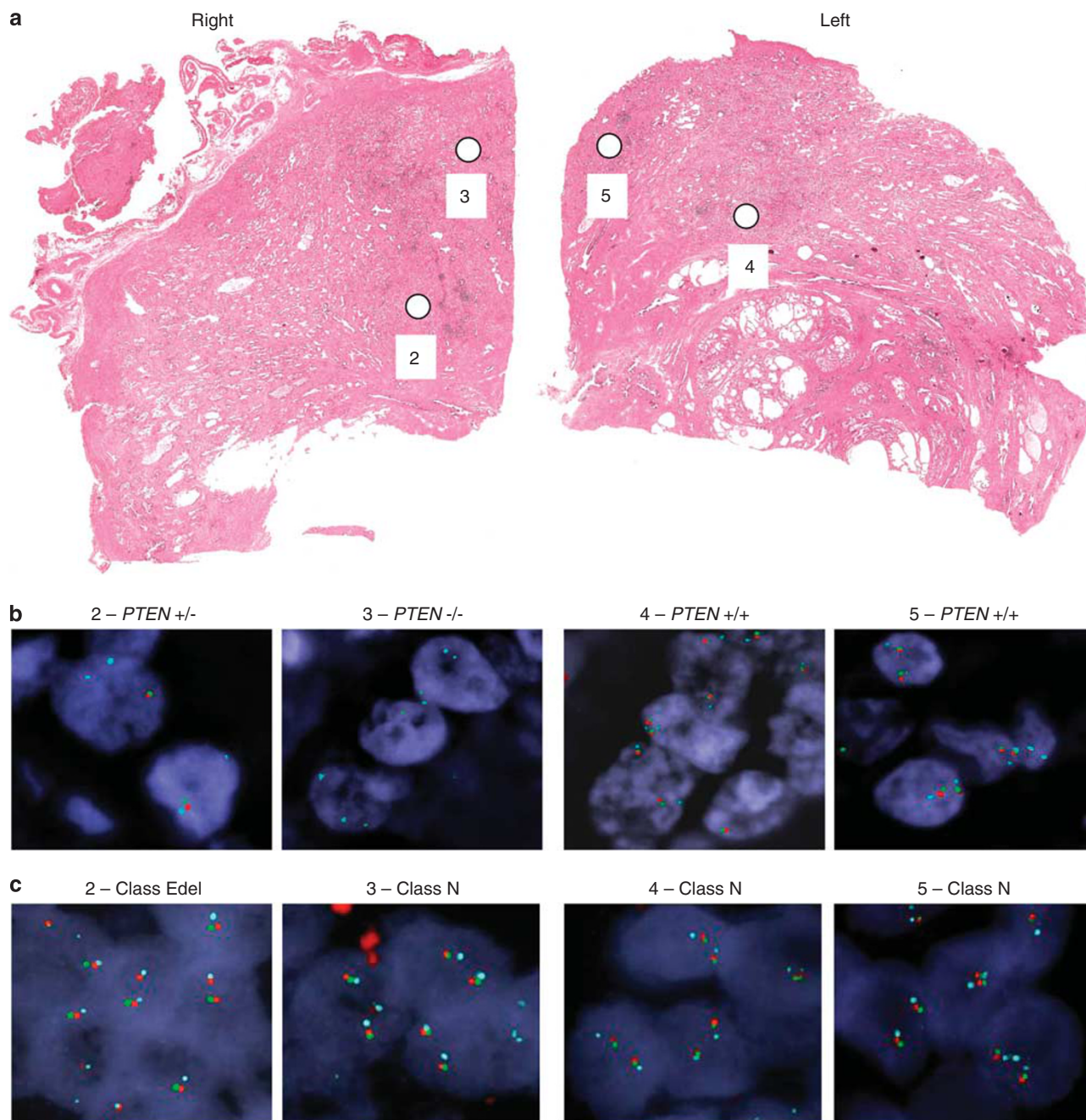


**Figure 3** Representative example of phosphatase and tensin homolog deleted on chromosome 10 (*PTEN*) heterogeneity in multifocal prostate cancer. (a) Hematoxylin and eosin sections from the right and left posterior quadrants of a radical prostatectomy specimen, with separate foci of adenocarcinoma showing the locations from which tissue microarray (TMA) cores were obtained. (b) Representative fluorescence *in situ* hybridization (FISH) images are shown for prostate cancer TMA applying the three-color *PTEN* FISH. The panel shows a pseudo-color image with the DAPI (4',6-diamidino-2-phenylindole, dihydrochloride)-counterstained nuclei. The original magnification is  $\times 63$ . The FISH image on the left shows tumor cells, focus 2—Gleason 3, with single signal for *PTEN* (red) and *FAS* (green) loci in most of the nuclei, and retained paired signals for CEP10 (pale blue), indicating hemizygous deletion of the *PTEN* gene region in prostate cancer. The following representative *PTEN* FISH image (foci 4 and 5, Gleason 3) shows homozygous *PTEN* deletion in prostate cancer, focus 3—Gleason 4, with absence of red signal for *PTEN* locus in most of the nuclei. The retained single green signal (*FAS* locus) in most of the nuclei and paired blue signals for CEP10 indicates hemizygous deletion of the *FAS* locus in focus 3. The last two FISH images (on the left) shows two signals of red (*PTEN* locus), green (*FAS* locus), as well as paired pale blue (CEP10) signals in most of the nuclei, indicating no deletion of *PTEN*. (c) Representative FISH images are shown for prostate cancer TMA applying the three-color *TMPRSS2-ERG* FISH. The FISH image on the left represents the prostate cancer focus 2 showing a Class Ed. The following images represent the foci 3, 4 and 5 with Class N configuration.



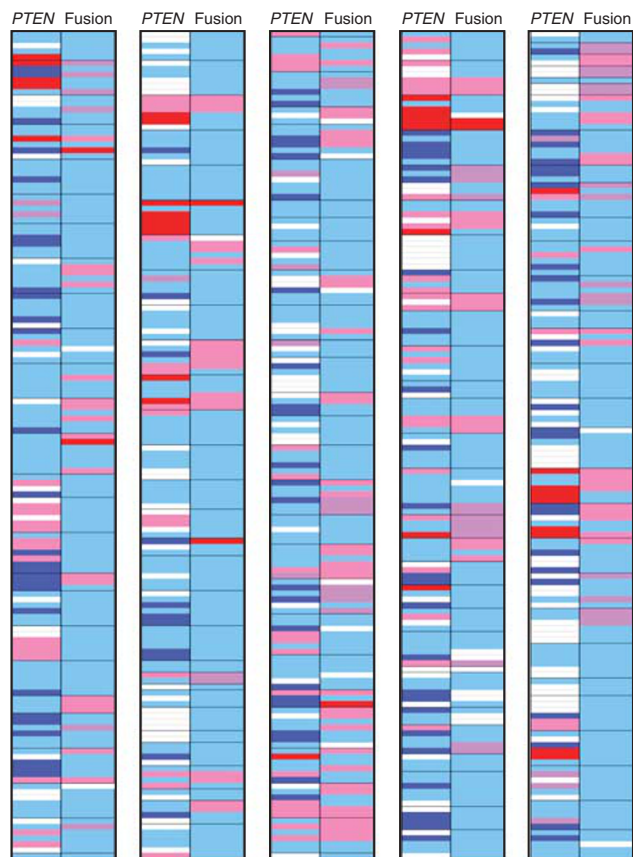


**Figure 4** Overall level of genetic heterogeneity of phosphatase and tensin homolog deleted on chromosome 10 (*PTEN*) deletion and *TMPRSS2-ERG* fusion within the cohort. The colored graph allows for a direct comparison of the pattern genetic diversity for *PTEN* deletion with that observed for *TMPRSS2-ERG* fusion. The color scheme used to represent the differential status of *PTEN* are as follows: not deleted = pale blue; hemizygous deletion = pale pink; homozygous deletion = red; monosomy of chromosome 10 = purple; gain of chromosome 10 = blue; not suitable for fluorescence *in situ* hybridization (FISH) = white. The color scheme used to represent the differential status of *TMPRSS2-ERG* fusion are as follows: absence of fusion = pale blue; Edel = pale pink; 2 + Edel (duplicated fusions) = red; Esplit = purple; gain of chromosome 21 = blue; not suitable for FISH = white.

multifocal prostate cancer could provide valuable insight into the problem of identifying the clinically relevant focus. In fact, there is evidence from several studies that smaller cancer foci harboring allelic losses on chromosomes 8p, 10q and 16q, *MYC* amplification and *PTEN* deletions possess metastatic potential not shown by larger foci without these changes.<sup>69–71</sup> However, a recent report from Guo *et al*<sup>72</sup> showed complete concordance between the presence of *TMPRSS2-ERG* gene rearrangements in metastatic deposits in pelvic lymph nodes and those found in the largest tumor focus. As such, it is likely that defining the index tumor will require consideration of size, Gleason score, pathologic stage and genomic changes.

Multifocal prostate cancer could potentially arise from divergent clones derived from one progenitor, from ‘field cancerization’ or from generalized

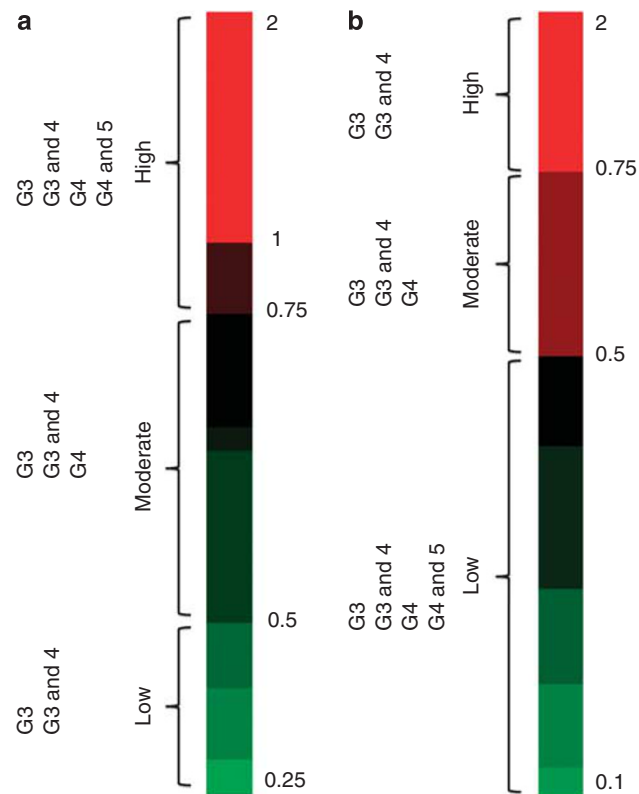


**Figure 5** Representation of phosphatase and tensin homolog deleted on chromosome 10 (*PTEN*) and *TMPRSS2-ERG* fluorescence *in situ* hybridization (FISH) patterns observed in different Gleason scores. The colored rectangles in a matrix represent the heterogeneity index, which was obtained as follows: number of different foci divided by number of different FISH results. The color scheme used to represent heterogeneity level is red or green (red for high level, green for low level of heterogeneity), and the intensity varies according to the range presented by *PTEN* and *TMPRSS2-ERG* FISH results. (a) Each row represents the heterogeneity index of *PTEN* FISH patterns across all cores from a single case. The color scheme ranges from 0.25 to 2. (b) Each row represents the heterogeneity index of *TMPRSS2-ERG* FISH patterns across all cores from a single case. The color scheme ranges from 0.1 to 2.

genotoxic damage (reviewed in Squire *et al*<sup>19</sup>). On the basis of allelic imbalance, Bostwick *et al*<sup>62</sup> and others<sup>73–75</sup> showed that separate foci in multifocal disease foci likely arise independently. This concept was confirmed later by analyses of *TMPRSS2-ETS* fusion genes in whole-mount prostatectomy specimens.<sup>76</sup> Mehra *et al*,<sup>54</sup> using FISH to classify *TMPRSS2* rearrangements by type, also suggested that individual foci have distinct rearrangements. Overall, 70% of the tumors in the Mehra study showed *TMPRSS2* rearrangement, including 63% through deletion, 27% through translocation and 10% through both mechanisms in separate tumor foci. Of the *TMPRSS2*-rearranged cases, 30% showed concordance in all tumor foci within a given prostate, whereas 70% were discordant in at least one focus. These findings demonstrate that multifocal prostate cancer appears to be a

heterogeneous disease at the genetic level, arising from multiple, independent clonal expansions within the gland (reviewed in Andreou and Cheng<sup>3</sup>).

The clinical significance of *PTEN* deletions and *TMPRSS2* rearrangements in prostate cancer has been well studied, with clinical relevance of the latter being unclear at best. *TMPRSS2* rearrangements seem to be reproducibly associated with a less favorable prognosis only when accompanied by *PTEN* loss.<sup>14,39</sup> The present study was not designed to further assess the association between *PTEN* deletions, *TMPRSS2-ERG* rearrangements and clinical outcome. Rather, the aim was to define the incidence of heterogeneity for *PTEN* deletions and *TMPRSS2-ERG* fusion rearrangements within and between separate cancer foci in the same prostate, and to determine whether there was any association with modified Gleason pattern. To this end, we studied a typical radical prostatectomy cohort in which 79% of the prostates contained multifocal disease. In 4% of cases, genomic heterogeneity was evident with both hemi- and homozygous *PTEN* deletions being observed in separate foci in the same prostate. Uniform mechanisms of deletion were seen

in all foci in only 9% of cases with a deletion. In 7% of cases, *TMPRSS2-ERG* fusion gene was present in at least one tumor focus, whereas 55% of cases appeared to have no *TMPRSS2* fusion gene in any tumor foci. In only one case was genomic heterogeneity evident with both mechanisms of the *TMPRSS2-ERG* fusion gene rearrangement in separate tumor foci. However, in *TMPRSS2-ERG* fusion-positive cases, the same mechanism of fusion gene formation was seen in all tumor foci in 15% of cases. We observed Edel *TMPRSS2* fusion genes in 29% of the cases and Esplit *TMPRSS2-ERG* fusion genes in 15% of the cases. In 24% of the cases examined by both FISH assays, there was *PTEN* loss and concurrent presence of a *TMPRSS2-ERG* fusion gene.

Overall heterogeneity for the *TMPRSS2* rearrangement between individual tumor foci was common; however, individual tumor cells within a given focus were homogeneous for *TMPRSS2* rearrangements. These findings are consistent with previous observations,<sup>54</sup> suggesting that individual tumor foci develop through clonal expansion. In addition, FISH analysis of the *TMPRSS2-ERG* fusion identified one cancer focus with two distinct rearrangements on the left side of the gland (Edel in one focus and Esplit in another focus). As such, the findings of this study support the hypothesis that multifocality and morphologic heterogeneity in prostate cancer is a result of independent malignancies with distinct clonal origins. When different tumor foci from individual prostatectomy specimens were compared with respect to *PTEN* deletion, striking heterogeneity between and within separate tumor foci was found. Our results suggest that this genetic heterogeneity may be an underlying molecular mechanism for diverse clinical and morphologic manifestations of prostate cancer. Our observations concerning heterogeneity of *PTEN* and *TMPRSS2-ERG* in multifocal prostate cancer have practical implications for personalized medicine. This particularly applies to the clinical use of *PTEN* FISH as a prognostic tool in prostatectomy specimens and site-directed needle biopsies. Our findings suggest that each cancer focus in a prostatectomy specimen with multifocal disease would need to be analyzed, to obtain accurate information on *PTEN* status. Similarly, each positive core in a set of site-directed needle biopsies should be assessed. With prostate biopsies, it is important to note that finding non-deleted *PTEN* cancer may be

**Table 4** Analysis of *PTEN* and *TMPRSS2-ERG* FISH results based on TMA cores

| FISH results                    | Grade    |          |
|---------------------------------|----------|----------|
|                                 | 3        | 4        |
| <i>PTEN</i> <sup>a</sup>        |          |          |
| Not deleted, n = 452 (%)        | 354 (78) | 97 (22)  |
| Hemizygous del, n = 85 (%)      | 51 (60)  | 34 (40)  |
| Homozygous del, n = 31 (%)      | 12 (39)  | 19 (61)  |
| P-value                         | —        | <0.001   |
| <i>TMPRSS2-ERG</i> <sup>a</sup> |          |          |
| Class N, n = 535 (%)            | 390 (75) | 127 (25) |
| Class Edel, n = 107 (%)         | 76 (71)  | 31 (29)  |
| Class Esplit, n = 48 (%)        | 40 (83)  | 8 (17)   |
| P-value                         | —        | 0.257    |

Abbreviations: del: deletion; FISH, fluorescence *in situ* hybridization; *PTEN*, phosphatase and tensin homolog deleted on chromosome 10; TMA, tissue microarray.

$\chi^2$ -analysis showed greater-than-expected association between *PTEN* loss and Gleason grade 4, and no association between presence or absence of fusion gene and Gleason pattern.

<sup>a</sup>*PTEN* and *TMPRSS2-ERG* FISH analyses were not suitable for all 692 cores.

**Table 5** Analysis of *TMPRSS2-ERG* FISH results based on TMA cores

| Variable    | Category       | Class N, n = 535 (%) | Class Edel, n = 107 (%) | Class Esplit, n = 48 (%) | P-value |
|-------------|----------------|----------------------|-------------------------|--------------------------|---------|
| <i>PTEN</i> | Not deleted    | 338 (82)             | 62 (67)                 | 33 (79)                  | —       |
|             | Hemizygous del | 54 (13)              | 26 (28)                 | 5 (12)                   | —       |
|             | Homozygous del | 21 (5)               | 5 (5)                   | 4 (10)                   | 0.007   |

Abbreviations: del, deletion; FISH, fluorescence *in situ* hybridization; *PTEN*, phosphatase and tensin homolog deleted on chromosome 10.  $\chi^2$ -analysis showed greater-than-expected association between *PTEN* loss and presence of fusion gene.

of limited value in terms of reassuring a patient that his prostate cancer could be less aggressive, as needle biopsies could fail to sample areas of cancer that have undergone *PTEN* deletion. Conversely, finding *PTEN* deletion (hemizygous or homozygous) in biopsies may be more robust in terms of predicting more aggressive tumor behavior and suggesting that a given patient not opt to go on active surveillance. Specific outcome studies using prostate biopsies, either prospective or retrospective, will be required to confirm this impression.

## Acknowledgements

This study was entirely funded by a grant to AJE (principle investigator) from the Ontario Institute for Cancer Research. We thank Ms Karen Hersey and Ms Roni Sambas for administrative and secretarial support, respectively.

## Disclosure/conflict of interest

JS has consulted for CymoGenDx LLC. All other authors declare no conflict of interest.

## References

- Nwosu V, Carpten J, Trent JM, *et al*. Heterogeneity of genetic alterations in prostate cancer: evidence of the complex nature of the disease. *Hum Mol Genet* 2001;10:2313–2318.
- Huland H, Graefen M, Haese A, *et al*. Prediction of tumor heterogeneity in localized prostate cancer. *Urol Clin North Am* 2002;29:213–222.
- Andreoiu M, Cheng L. Multifocal prostate cancer: biologic, prognostic, and therapeutic implications. *Hum Pathol* 2010;41:781–793.
- Grignon DJ. Unusual subtypes of prostate cancer. *Mod Pathol* 2004;17:316–327.
- Wise AM, Stamey TA, McNeal JE, *et al*. Morphologic and clinical significance of multifocal prostate cancers in radical prostatectomy specimens. *Urology* 2002;60:264–269.
- Villers A, McNeal JE, Freiha FS, *et al*. Multiple cancers in the prostate. Morphologic features of clinically recognized versus incidental tumors. *Cancer* 1992;70:2313–2318.
- Allsbrook WC Jr, Mangold KA, Johnson MH, *et al*. Interobserver reproducibility of Gleason grading of prostatic carcinoma: general pathologist. *Hum Pathol* 2001;32:81–88.
- Epstein JI, Allsbrook WC Jr, Amin MB, *et al*. The 2005 International Society of Urological Pathology (ISUP) Consensus Conference on Gleason Grading of Prostatic Carcinoma. *Am J Surg Pathol* 2005;29:1228–1242.
- Arora R, Koch MO, Eble JN, *et al*. Heterogeneity of Gleason grade in multifocal adenocarcinoma of the prostate. *Cancer* 2004;100:2362–2366.
- Fleshner N. Defining high-risk prostate cancer: current status. *Can J Urol* 2005;12(Suppl 1):14–17; discussion 94–6.
- Klotz L. Active surveillance with selective delayed intervention using PSA doubling time for good risk prostate cancer. *Eur Urol* 2005;47:16–21.
- Shen MM, Abate-Shen C. Molecular genetics of prostate cancer: new prospects for old challenges. *Genes Dev* 2010;24:1967–2000.
- Tomlins SA, Rhodes DR, Perner S, *et al*. Recurrent fusion of TMPRSS2 and ETS transcription factor genes in prostate cancer. *Science* 2005;310:644–648.
- Yoshimoto M, Joshua AM, Cunha IW, *et al*. Absence of TMPRSS2:ERG fusions and PTEN losses in prostate cancer is associated with a favorable outcome. *Mod Pathol* 2008;21:1451–1460.
- Yoshimoto M, Ludkovski O, Bayani J, *et al*. Microdeletion and concurrent translocation associated with a complex TMPRSS2:ERG prostate cancer gene fusion. *Genes Chromosomes Cancer* 2007;46:861–863.
- Braun M, Scheble VJ, Menon R, *et al*. Relevance of cohort design for studying the frequency of the ERG rearrangement in prostate cancer. *Histopathology* 2011;58:1028–1036.
- Joshua AM, Evans A, Van der Kwast T, *et al*. Prostatic preneoplasia and beyond. *Biochim Biophys Acta* 2008;1785:156–181.
- Mehra R, Tomlins SA, Yu J, *et al*. Characterization of TMPRSS2-ETS gene aberrations in androgen-independent metastatic prostate cancer. *Cancer Res* 2008;68:3584–3590.
- Squire JA, Park PC, Yoshimoto M, *et al*. Prostate cancer as a model system for genetic diversity in tumors. *Adv Cancer Res* 2011;112:183–216.
- Squire JA. TMPRSS2-ERG and PTEN loss in prostate cancer. *Nat Genet* 2009;41:509–510.
- Mosquera JM, Mehra R, Regan MM, *et al*. Prevalence of TMPRSS2-ERG fusion prostate cancer among men undergoing prostate biopsy in the United States. *Clin Cancer Res* 2009;15:4706–4711.
- Magi-Galluzzi C, Tsusuki T, Elson P, *et al*. TMPRSS2-ERG gene fusion prevalence and class are significantly different in prostate cancer of Caucasian, African-American and Japanese patients. *Prostate* 2011;71:489–497.
- Furusato B, Tan SH, Young D, *et al*. ERG oncoprotein expression in prostate cancer: clonal progression of ERG-positive tumor cells and potential for ERG-based stratification. *Prostate Cancer Prostatic Dis* 2010;13:228–237.
- Ellett F, Kile BT, Lieschke GJ. The role of the ETS factor ERG in zebrafish vasculogenesis. *Mech Dev* 2009;126:220–229.
- Hawksworth D, Ravindranath L, Chen Y, *et al*. Overexpression of C-MYC oncogene in prostate cancer predicts biochemical recurrence. *Prostate Cancer Prostatic Dis* 2010;13:311–315.
- Schulz WA, Ingenwerth M, Djuidje CE, *et al*. Changes in cortical cytoskeletal and extracellular matrix gene expression in prostate cancer are related to oncogenic ERG deregulation. *BMC Cancer* 2010;10:505.
- Singh S, Barrett J, Sakata K, *et al*. ETS proteins and MMPs: partners in invasion and metastasis. *Curr Drug Targets* 2002;3:359–367.
- Zhang S, Yu D. PI(3)kinase apart PTEN's role in cancer. *Clin Cancer Res* 2010;16:4325–4330.
- Feilotter HE, Nagai MA, Boag AH, *et al*. Analysis of PTEN and the 10q23 region in primary prostate carcinomas. *Oncogene* 1998;16:1743–1748.

- 30 Muller M, Rink K, Krause H, *et al*. PTEN/MMAC1 mutations in prostate cancer. *Prostate Cancer Prostatic Dis* 2000;3:S32.
- 31 Verhagen PC, van Duijn PW, Hermans KG, *et al*. The PTEN gene in locally progressive prostate cancer is preferentially inactivated by bi-allelic gene deletion. *J Pathol* 2006;208:699–707.
- 32 Bednarz N, Eltze E, Semjonow A, *et al*. BRCA1 loss preexisting in small subpopulations of prostate cancer is associated with advanced disease and metastatic spread to lymph nodes and peripheral blood. *Clin Cancer Res* 2010;16:3340–3348.
- 33 Bismar TA, Yoshimoto M, Vollmer RT, *et al*. PTEN genomic deletion is an early event associated with ERG gene rearrangements in prostate cancer. *BJU Int* 2011;107:477–485.
- 34 Hermans KG, van Alewijk DC, Veltman JA, *et al*. Loss of a small region around the PTEN locus is a major chromosome 10 alteration in prostate cancer xenografts and cell lines. *Genes Chromosomes Cancer* 2004;39:171–184.
- 35 Ishkanian AS, Malloff CA, Ho J, *et al*. High-resolution array CGH identifies novel regions of genomic alteration in intermediate-risk prostate cancer. *Prostate* 2009;69:1091–1100.
- 36 Lapointe J, Li C, Giacomini CP, *et al*. Genomic profiling reveals alternative genetic pathways of prostate tumorigenesis. *Cancer Res* 2007;67:8504–8510.
- 37 Yoshimoto M, Cunha IW, Coudry RA, *et al*. FISH analysis of 107 prostate cancers shows that PTEN genomic deletion is associated with poor clinical outcome. *Br J Cancer* 2007;97:678–685.
- 38 Yoshimoto M, Cutz JC, Nuin PA, *et al*. Interphase FISH analysis of PTEN in histologic sections shows genomic deletions in 68% of primary prostate cancer and 23% of high-grade prostatic intra-epithelial neoplasias. *Cancer Genet Cytogenet* 2006;169:128–137.
- 39 Reid AH, Attard G, Ambroisine L, *et al*. Molecular characterisation of ERG, ETV1 and PTEN gene loci identifies patients at low and high risk of death from prostate cancer. *Br J Cancer* 2010;102:678–684.
- 40 Sircar K, Yoshimoto M, Monzon FA, *et al*. PTEN genomic deletion is associated with p-Akt and AR signalling in poorer outcome, hormone refractory prostate cancer. *J Pathol* 2009;218:505–513.
- 41 Taylor BS, Schultz N, Hieronymus H, *et al*. Integrative genomic profiling of human prostate cancer. *Cancer Cell* 2010;18:11–22.
- 42 Holcomb IN, Young JM, Coleman IM, *et al*. Comparative analyses of chromosome alterations in soft-tissue metastases within and across patients with castration-resistant prostate cancer. *Cancer Res* 2009;69:7793–7802.
- 43 Liu W, Laitinen S, Khan S, *et al*. Copy number analysis indicates monoclonal origin of lethal metastatic prostate cancer. *Nat Med* 2009;15:559–565.
- 44 Yoshimoto M, Ludkovski O, Degrace D, *et al*. PTEN genomic deletions that characterize aggressive prostate cancer originate close to segmental duplications. *Genes Chromosomes Cancer* 2012;51:149–160.
- 45 McMenamin ME, Soung P, Perera S, *et al*. Loss of PTEN expression in paraffin-embedded primary prostate cancer correlates with high Gleason score and advanced stage. *Cancer Res* 1999;59:4291–4296.
- 46 Schmitz M, Grignard G, Margue C, *et al*. Complete loss of PTEN expression as a possible early prognostic marker for prostate cancer metastasis. *Int J Cancer* 2007;120:1284–1292.
- 47 Carver BS, Tran J, Gopalan A, *et al*. Aberrant ERG expression cooperates with loss of PTEN to promote cancer progression in the prostate. *Nat Genet* 2009;41:619–624.
- 48 Sarker D, Reid AH, Yap TA, *et al*. Targeting the PI3K/AKT pathway for the treatment of prostate cancer. *Clin Cancer Res* 2009;15:4799–4805.
- 49 Koksall IT, Dirice E, Yasar D, *et al*. The assessment of PTEN tumor suppressor gene in combination with Gleason scoring and serum PSA to evaluate progression of prostate carcinoma. *Urol Oncol* 2004;22:307–312.
- 50 Ayala G, Thompson T, Yang G, *et al*. High levels of phosphorylated form of Akt-1 in prostate cancer and non-neoplastic prostate tissues are strong predictors of biochemical recurrence. *Clin Cancer Res* 2004;10:6572–6578.
- 51 Ohgashi T, Mizuno R, Nakashima J, *et al*. Inhibition of Wnt signaling downregulates Akt activity and induces chemosensitivity in PTEN-mutated prostate cancer cells. *Prostate* 2005;62:61–68.
- 52 Wang Y, Romigh T, He X, *et al*. Resveratrol regulates the PTEN/AKT pathway through androgen receptor-dependent and -independent mechanisms in prostate cancer cell lines. *Hum Mol Genet* 2010;19:4319–4329.
- 53 Barry M, Perner S, Demichelis F, *et al*. TMPRSS2-ERG fusion heterogeneity in multifocal prostate cancer: clinical and biologic implications. *Urology* 2007;70:630–633.
- 54 Mehra R, Han B, Tomlins SA, *et al*. Heterogeneity of TMPRSS2 gene rearrangements in multifocal prostate adenocarcinoma: molecular evidence for an independent group of diseases. *Cancer Res* 2007;67:7991–7995.
- 55 Ventura RA, Martin-Subero JI, Jones M, *et al*. FISH analysis for the detection of lymphoma-associated chromosomal abnormalities in routine paraffin-embedded tissue. *J Mol Diagn* 2006;8:141–151.
- 56 Attard G, Swennenhuis JF, Olmos D, *et al*. Characterization of ERG, AR and PTEN gene status in circulating tumor cells from patients with castration-resistant prostate cancer. *Cancer Res* 2009;69:2912–2918.
- 57 Kawai T, Hiroi S, Nakanishi K, *et al*. Abnormalities in chromosome 17 and p53 in lung carcinoma cells detected by fluorescence *in situ* hybridization. *Pathol Int* 2004;54:413–419.
- 58 Korshunov A, Sycheva R, Gorelyshev S, *et al*. Clinical utility of fluorescence *in situ* hybridization (FISH) in nonbrainstem glioblastomas of childhood. *Mod Pathol* 2005;18:1258–1263.
- 59 Mezzelani A, Alasio L, Bartoli C, *et al*. c-erbB2/neu gene and chromosome 17 analysis in breast cancer by FISH on archival cytological fine-needle aspirates. *Br J Cancer* 1999;80:519–525.
- 60 Fujii H, Ajioka Y, Kazami S, *et al*. Loss of heterozygosity in the clonal evolution of flat colorectal neoplasms. *J Pathol* 2002;197:298–306.
- 61 Saeed AI, Sharov V, White J, *et al*. TM4: a free, open-source system for microarray data management and analysis. *Biotechniques* 2003;34:374–378.
- 62 Bostwick DG, Shan A, Qian J, *et al*. Independent origin of multiple foci of prostatic intraepithelial neoplasia: comparison with matched foci of prostate carcinoma. *Cancer* 1998;83:1995–2002.
- 63 Ruijter ET, van de Kaa CA, Schalken JA, *et al*. Histological grade heterogeneity in multifocal prostate cancer. Biological and clinical implications. *J Pathol* 1996;180:295–299.

- 64 Greene DR, Wheeler TM, Egawa S, *et al*. A comparison of the morphological features of cancer arising in the transition zone and in the peripheral zone of the prostate. *J Urol* 1991;146:1069–1076.
- 65 Villers A, Abecassis R, Baron JC, *et al*. [Extraperitoneal endoscopic lymph node dissection with insufflation in the staging of bladder and prostate cancer]. *Prog Urol* 1992;2:892–900.
- 66 McNeal JE, Price HM, Redwine EA, *et al*. Stage A versus stage B adenocarcinoma of the prostate: morphological comparison and biological significance. *J Urol* 1988;139:61–65.
- 67 Stamey TA, McNeal JE, Yemoto CM, *et al*. Biological determinants of cancer progression in men with prostate cancer. *JAMA* 1999;281:1395–1400.
- 68 van der Kwast TH, Amin MB, Billis A, *et al*. International Society of Urological Pathology (ISUP) Consensus Conference on Handling and Staging of Radical Prostatectomy Specimens. Working group 2: T2 substaging and prostate cancer volume. *Mod Pathol* 2011;24:16–25.
- 69 Sakr WA, Macoska JA, Benson P, *et al*. Allelic loss in locally metastatic, multisampled prostate cancer. *Cancer Res* 1994;54:3273–3277.
- 70 Jenkins RB, Qian J, Lieber MM, *et al*. Detection of c-myc oncogene amplification and chromosomal anomalies in metastatic prostatic carcinoma by fluorescence *in situ* hybridization. *Cancer Res* 1997;57:524–531.
- 71 Schmidt H, DeAngelis G, Eltze E, *et al*. Asynchronous growth of prostate cancer is reflected by circulating tumor cells delivered from distinct, even small foci, harboring loss of heterozygosity of the PTEN gene. *Cancer Res* 2006;66:8959–8965.
- 72 Guo CC, Wang Y, Xiao L, *et al*. The relationship of TMPRSS2-ERG gene fusion between primary and metastatic prostate cancers. *Hum Pathol* 2012;43:644–649.
- 73 Cheng L, Song SY, Pretlow TG, *et al*. Evidence of independent origin of multiple tumors from patients with prostate cancer. *J Natl Cancer Inst* 1998;90:233–237.
- 74 Macintosh CA, Stower M, Reid N, *et al*. Precise microdissection of human prostate cancers reveals genotypic heterogeneity. *Cancer Res* 1998;58:23–28.
- 75 Ruijter ET, Miller GJ, van de Kaa CA, *et al*. Molecular analysis of multifocal prostate cancer lesions. *J Pathol* 1999;188:271–277.
- 76 Furusato B, Gao CL, Ravindranath L, *et al*. Mapping of TMPRSS2-ERG fusions in the context of multi-focal prostate cancer. *Mod Pathol* 2008;21:67–75.

Supplementary information accompanies the paper on Modern Pathology website (<http://www.nature.com/modpathol>)